Interplay of RKKY, Zeeman, and Dzyaloshinskii-Moriya interactions and the nonzero average spin chirality in Dy/Y multilayer structures

S. V. Grigoriev,[1,*] D. Lott,[2] Yu. O. Chetverikov,[1] A. T. D. Grünwald,[2] R. C. C. Ward,[3] and A. Schreyer[2]
[1]*Petersburg Nuclear Physics Institute, Gatchina, St. Petersburg 188300, Russia*
[2]*GKSS Research Centre, 21502 Geesthacht, Germany*
[3]*Oxford Physics, Clarendon Laboratory, Parks Road, Oxford OX1 3PU, United Kingdom*
(Received 13 July 2010; published 16 November 2010)

Metal magnetic/nonmagnetic (Dy/Y) multilayer structures posses a coherent spin helix propagating through many Dy/Y bilayers. Samples of different Dy and Y layer thicknesses were investigated using polarized neutron scattering to determine the average chirality of the magnetic structure. The in-plane applied magnetic field induces the chirality since it couples to the uncompensated moments of the helix in a Dy layer. The value of the chirality has a complex behavior in dependence on the temperature and the magnetic field. It is shown that the chirality is affected by the competition between the Ruderman-Kittel-Kasuya-Yoshida interactions of the intralayer exchange within the Dy layers and the interlayer coupling across the nonmagnetic Y layers. The set of the experimental data allows one to make the reconstruction and schematic visualization of the spin structure within the multilayer system. In spite of a complex dependency of the average chirality on the temperature and the magnetic field, the twist angle between the spin planes of two neighboring Y/Dy interfaces has the same sign for all samples at any conditions. It is antisymmetric Dzyaloshinsky-Moriya interaction that reveals itself through the sign of this twist angle and as a result through the nonzero average chirality of the magnetic multilayer structure.

DOI: 10.1103/PhysRevB.82.195432 PACS number(s): 75.70.−i, 74.78.Fk

I. INTRODUCTION

The effect of giant magnetoresistance (GMR) in magnetic multilayer structures (MMLs) (Refs. 1 and 2) is one of the examples where the technical applications run ahead of the clear fundamental description of the underlying phenomena. The GMR effect describes the fact that structures consisting of ferromagnetic (F) and nonmagnetic layers can be coupled antiferromagnetically (AF) in zero field while the applied magnetic field results into a ferromagnetic configuration and in a multiple decrease in the electric resistance. The antiferromagnetic coupling is related to the oscillatory Ruderman-Kittel-Kasuya-Yoshida (RKKY) interaction with $J_{\perp} \sim \sin(dk_F)/(dk_F)^2$, where d is the thickness of the layer and k_F is the Fermi wave vector.[3] This interaction is determined by the topological properties of the Fermi surface of the nonmagnetic layer material. It was experimentally confirmed that the manipulation of the layer thickness or the value of k_F is indeed able to change the sign of the interaction.[4] Upon the application of an in-plane magnetic field a spin-flop transition occurs at H_{fl} which turns into a ferromagnetic phase at H_{fm}. The spin-flop transition at the surface appears at a field which is a factor of $\sqrt{2}$ smaller as it is observed in their bulk constituents.[5] A more detailed study of the spin-flop phase using polarized neutron reflectometry (PNR) has demonstrated the nonuniformly twisted, canted state in the MML in the spin-flop phase. The canting angles are maximal in the terminal layers and progressively relax toward the middle of the MML from both sides.[6]

Although the mechanism of the interlayer bilinear coupling ascribed to the RKKY interaction is well established, an additional interaction, the so-called biquadratic coupling remains open for discussion.[7–15] The biquadratic coupling stabilizes the spin arrangement with a relative angle of 90° between the magnetizations of two neighboring ferromagnetic layers separated by a spacer layer while the bilinear coupling lead to an AF/F coupling with angles of 180°/0°. First experiments, revealing the 90° moment arrangement in trilayer Fe/Cr/Fe systems,[7] however, were explained via spatial fluctuations of the microscopic bilinear coupling[8] and thus reducing the observed biquadratic coupling as having a nonfundamental origin. Subsequent experiments with trilayers[9–11] were adequately explained within the same theory.[8] On the other hand, there are several papers insisting on the microscopic origin of the biquadratic coupling in multilayer systems.[12,13,15] Especially impressive is the work of Suenaga *et al.*,[15] where it is shown that (i) the biquadratic coupling in Fe/Cr multilayers is comparable to the RKKY for systems with large thickness of the Cr interlayer; (ii) the biquadratic coupling is connected to the GMR effect, and (iii) it can be affected by the application of high pressure. The conclusion on the enhancement of the biquadratic term is often based on magnetization measurements since the multilayer structures are inaccessible for magneto-optical methods. The magnetization curve, however, can sometimes mimic the presence of a strong biquadratic interlayer exchange coupling as it was shown for Fe/Si multilayers.[14] Here, PNR can play a decisive role for the visualization of the 90° moment arrangement. In conclusion of the introduction, three interactions responsible for the GMR effect in the MML structures are discussed: the RKKY interaction, the Zeeman interaction, and the interaction due to a weak biquadratic exchange coupling.

The observation of noncollinear magnetic structures in MML can be also a result of the Dzyaloshinskii-Moriya (DM) interaction induced by the broken symmetry at the interfaces between magnetic and nonmagnetic layers, as it was theoretically predicted in Refs. 16 and 17. The DM in-

teraction, similar to the biquadratic exchange coupling, promotes the noncollinear arrangement of adjacent ferromagnetic sheets of spins in the MMLs. The fingerprint of the DM interaction is the occurrence of spin arrangements with a certain chirality. However, it is in general difficult to detect and study the chirality in MMLs with ferromagnetic intralayer coupling. MMLs with spiral arrangements of the spins inside the magnetic layers (Dy, Ho, etc.) on the other hand are prime candidates to study this effect since the DM interaction causes, directly or indirectly, an imbalance of the population for either handedness.[18]

The magnetic layers of Dy/Y and Ho/Y MMLs are helically ordered below T_N due to the RKKY interaction within the layers (intralayer RKKY interaction). The pitch angles of the helicoidal structures in MMLs are comparable to the pitch angles of their magnetic bulk constituents (Dy or Ho), provided that the magnetic layers are sufficiently thick.[19–22] The major interaction that determines the magnetic structure of the entire MML is the RKKY interaction. It is the RKKY interaction between the Dy layers which is primarily related to the thickness of the Y layer with $k_F d_Y$, where the wave vector k_F is a temperature-independent quantity.[4,19] The in-plane applied magnetic field affects the MMLs spin structure on different energy scales: at first, when it reaches the strength of the relatively weak RKKY interaction between the magnetic layers at an applied magnetic field of 0.1–0.2 T, and further when it exceeds the strong RKKY interaction within the magnetic layer at about 1–2 T. In general, the applied magnetic field couples the uncompensated moments of the helix in a Dy layer via the Zeeman interaction. It varies considerably with the temperature and the magnetic field as a function of several parameters: (i) the strength of the applied field H; (ii) the uncompensated moments of the individual Dy layers which varies with the helix wave vector $k_{Dy}(T)$ and with the staggered magnetization $M(T)$.

Our previous measurements with polarized neutrons have demonstrated that Dy/Y MML structures posses a coherent helical spin structure over many bilayers with a predominant chirality induced by the in-plane applied magnetic field.[18] It was therefore suggested that the interplay of the RKKY and the Zeeman interactions helps to reveal the antisymmetric Dzyaloshinskii-Moriya interaction since the observed chirality is a fingerprint of the DM interaction resulting from the lack of the symmetry inversion at the interfaces.[16,23] The aim of this paper is to study the conditions when the interplay between RKKY and Zeeman interactions in the Dy/Y MMLs leads to a considerable change in their chirality. The variation in the interactions can be achieved by either changing the thicknesses of the Y layers or the Dy layers resulting in a drastic modification of the strength of the RKKY interaction or the Zeeman interaction, respectively.

Here we demonstrate by means of polarized neutron scattering that the chirality of the helix induced by the in-plane applied magnetic field upon cooling depends on the value of the RKKY versus Zeeman interactions. We have therefore compared two samples with different Dy at equal Y layer thicknesses and two samples at equal Dy but different Y layer thicknesses. It is shown that in spite of a complex dependency of the average chirality on the temperature and the magnetic field, the interaction of the DM type inducing the chirality has the same sign for all samples at any conditions.

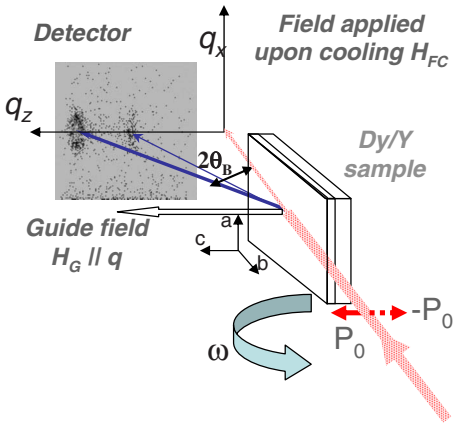

FIG. 1. (Color online) The schematic drawing of the experiment.

II. EXPERIMENTAL

The effect of an applied magnetic field on the chirality of the helix spin structure in MMLs was investigated at the following three samples: $[Dy_{3.0\ nm}/Y_{1.5\ nm}]_{150}$ (denoted Dy30/Y15) with T_N=155 K, $[Dy_{3.0\ nm}/Y_{3.0\ nm}]_{150}$ (denoted Dy30/Y30) with T_N=160 K, and $[Dy_{4.3\ nm}/Y_{3.0\ nm}]_{350}$ (denoted Dy42/Y30) with T_N=165 K. The samples were grown along the *c* axis [001] of the Dy and Y hcp structure by molecular-beam-epitaxy techniques. Below the Neél temperature, T_N, a coherent helical spin structure over several bilayers has been observed in agreement with previous findings.[19] Here, polarized neutrons are especially useful in the determination of the chirality of magnetic structures.[24] The total magnetic elastic neutron cross section for polarized neutrons can be separated into a spin-state-dependent contribution and a spin-state-independent part. The latter part is also asymmetric with respect to the momentum transfer **Q** and can be associated with the average chirality of the magnetic system.

The polarized neutron experiments were carried out at the neutron reflectometer, NeRo, at GKSS, using polarized neutrons of a wavelength of λ=0.435 nm at a $\Delta\lambda/\lambda$=0.02 and a polarization of P_0=0.975. The *c* axis of the multilayer sample was set almost perpendicular to the incident beam (Fig. 1). The sense of the polarization followed a guide magnetic field of 1 mT applied perpendicularly to the multilayer surface and thus pointed along the direction of the *c* axis of the Dy/Y lattice. This geometry was used to study the polarization-dependent part of the scattering cross section. In addition a magnetic field of up to 900 mT was applied along *z* direction and parallel to the multilayer surface. At this configuration with the polarization of the incident beam aligned along the direction of the applied field ($\mathbf{P}_0 \parallel \mathbf{Q}$), the corresponding scattered intensities, $[I^+ = I(\mathbf{Q}, +P_0)$ and $I^- = I(\mathbf{Q}, -P_0)]$, are related each to either of the right- and left-handed domains, respectively. The average chirality, which is proportional to the difference in the population of left- and right-handed helices, was measured as the polarization-dependent

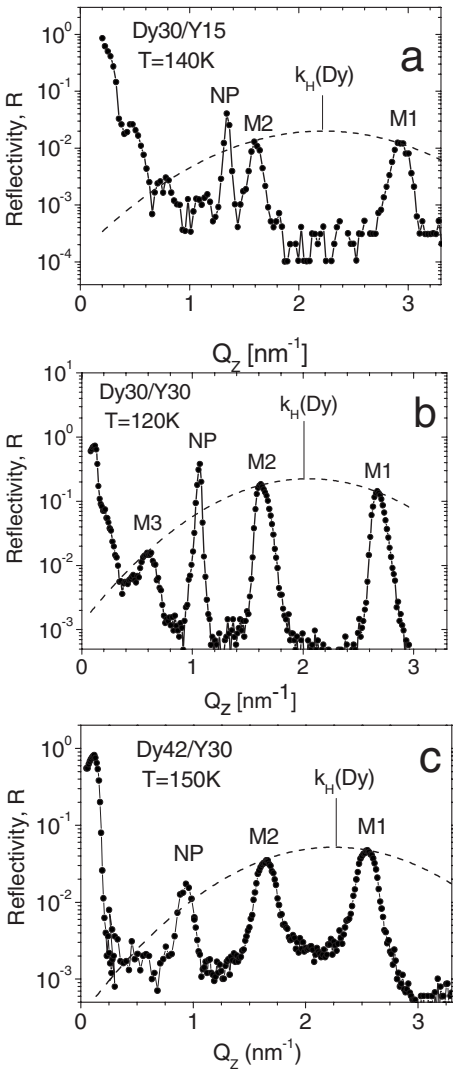

FIG. 2. The q dependence of the neutron-scattering intensity (reflectivity profile) for three samples (a) Dy30/Y15 taken at $T=130$ K, (b) Dy30/Y30 taken at $T=130$ K, and (c) Dy42/Y30 taken at $T=130$ K. NP is the nuclear peak, and M0 and M1 are the magnetic peaks.

asymmetric part of the magnetic neutron-scattering cross section.[18] We thus introduce here a chiral parameter directly related to the measured intensities and the imbalance between the left- and right-handed domains,

$$\gamma = \frac{(I^+ - I^-)}{(I^+ + I^-)}.$$

III. RESULTS

The specular reflectivity curves for the three samples [(a) Dy30/Y15, (b) Dy30/Y30, and (c) Dy42/Y30] taken below T_N are shown in Fig. 2. The nuclear peaks originating from the multilayer structure with the period lengths equal to the thicknesses of the Dy/Y bilayers of $d=d_{\mathrm{Dy}}+d_{\mathrm{Y}}=4.5$, 6.2, and 7.1 nm appear at $Q_N=2\pi/d=1.35$, 1.01, and 0.89 nm^{-1} [Figs. 2(a)–2(c), respectively]. The positions of these peaks do not change with temperature giving the evidence of their nuclear nature. The peaks at higher Q values, denoted as M1 and M2, respectively, and positioned at Q_{M1} and Q_{M2}, originate from helical spin structures and appear below T_N. The coexistence of additional magnetic satellite reflections is due to the modulation imposed by the nuclear multilayer structure on the spiral structure. Due to this modulation the magnetic peaks are separated in Q space by $(Q_{M1}-Q_{M2})=Q_N$.

The presence of clearly visible and well-separated peaks can be also interpreted in terms of the long-range correlation of the magnetic helix propagating through several bilayers. However, it is not trivial to extract the propagation vector of the helix in the sample from the data. As it was shown in Refs. 20–22, the data can be reasonably modeled if one suggests that the phase shift across the Y, associated with a wave vector k_{Y}, is different from the wave vector of Dy ($k_{\mathrm{Y}} \neq k_{\mathrm{Dy}}$). The result of the fit confirms that the value of k_{Y} of 3.1 nm^{-1} is temperature independent, corresponding to a turn angle between Y atomic planes along the c axis of 51° and hardly changes for the MMLs with different Y layer thickness (see page 5596 of Ref. 22). The wave vector within the Dy layers on the other hand decrease with temperature from $k_{\mathrm{Dy}}=2.5$ nm^{-1} close to T_N to 2.0 nm^{-1} around $T \sim 100$ K. Below 100 K it saturates upon further decrease in the temperature. The wave vectors of the helices were simply determined by assuming that the intensities of the magnetic peaks are modulated by the form factor of the Dy layer. By assuming a Gaussian function the value of k_{Dy} is given by its center position (see Fig. 2).

Rocking scans at the Bragg peak positions of the helices were taken at different temperatures after field cooling (FC) the sample at different values of the magnetic field H. Figure 3 shows rocking scans for the sample Dy30/Y15 after FC at $H=900$ mT down to $T=100$ K and $T=150$ K, respectively, taken at the peak position M1 and at a field of $H=0$. The rocking scans give an example of the nonzero difference between the two scattering intensities of opposite polarizations, I^+ and I^-, demonstrating the nonequal population of the left- and right-handed domains, i.e., the appearance of the nonzero average chirality in the sample.

Figure 4 shows the value of γ for the three samples [(a) Dy30/Y15, (b) Dy30/Y30, and (c) Dy42/Y30, respectively] for different temperature and magnetic field histories. In order to study the effect of the magnetic field on the chirality, the sample was first cooled from $T>T_N$ to $T<T_N$ in an in-plane field H. Thereupon the field was switched off and the γ value was measured in a small guide field, H_g, with $\mathbf{H}_g \| \mathbf{P}_0 \| \mathbf{k}$. For all three samples the FC procedure at $H=900$ mT down to temperatures close to $T=145$ K leads to a chirality of the same sign. For FC below $T=140$ K at the same magnetic field, the chirality remains positive for the sample Dy42/Y30, but becomes negative for the samples Dy30/Y30 and Dy30/Y15, respectively. Thus, it can be concluded preliminarily that the field-induced chirality depends on the thickness of the Dy layers. As it will be shown in the following it depends on the value of the phase factor of the helix $k_{\mathrm{Dy}}d_{\mathrm{Dy}}$ within one Dy layer. In relatively large magnetic fields in the order of 1 T, the chirality is positive when $k_{\mathrm{Dy}}d_{\mathrm{Dy}}>2\pi$, and negative when $k_{\mathrm{Dy}}d_{\mathrm{Dy}}<2\pi$.

An interesting behavior of the chirality factor γ is observed when the samples were first cooled at a field of H

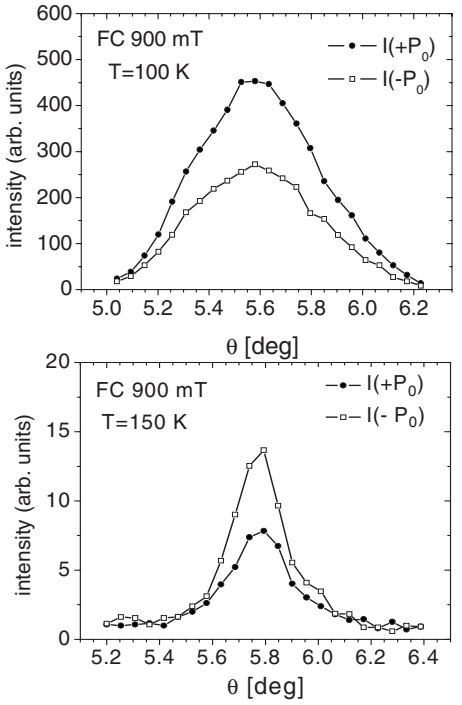

FIG. 3. The rocking scans $I(\omega)$ of the peak M1 [(a) after FC to 110 K and (b) 150 K and at $H=900$ mT) taken for two opposite polarizations at $H=1$ mT ($\mathbf{H}\|\mathbf{P_0}\|\mathbf{q}$).

$=900$ mT from above $T>T_N$ to $T=110$ K and thereafter the chirality was measured for different temperatures by subsequently warming up in zero field (Fig. 4). In this case the chirality (positive or negative) increases in its absolute value upon approaching T_N for the samples Dy42/Y30 and Dy30/Y30 but it decreases to zero for the sample Dy30/Y15. This behavior is obviously related to the difference in the thicknesses of the Y layer in the Dy/Y bilayers of the Dy/Y superlattices. Thus, for $d_Y=3$ nm the RKKY interaction between the Dy layers leads to a ferromagnetic type of coupling, as it is of antiferromagnetic nature for $d_Y=1.5$ nm. It should be noted that for zero FC (ZFC) the chirality factor γ is close to zero for Dy30/Y15 and Dy30/Y30 but equals to -0.10 for Dy42/Y30 in the whole temperature range below T_N. The enhancement of spontaneous chirality in the latter sample and its absence in the others are related to a misalignment of the crystallographic c axis of the grown single crystal and the film normal. A detailed description and interpretation of the phenomenon will be published elsewhere.[25]

Furthermore, it should be noted that the value of γ depends on the strength of the magnetic field applied in the sample plane (ab) during the FC procedure but not on its direction ($\pm\mathbf{H}_{FC}$). Figure 5 gives γ as a function of the magnetic field for all three samples [(a) Dy30/Y15, (b) Dy30/Y30, and (c) Dy42/Y30, respectively) taken at $T=110$ K, 130 K, and 150 K, respectively. The chiral parameter γ for the sample Dy42/Y30 increases in its absolute value with the increase in the magnetic field during FC for all three temperatures [Fig. 5(c)]. On the other hand, the chirality factor γ for the sample Dy30/Y30 show opposite signs upon the increase in the magnetic field during FC for the subcritical

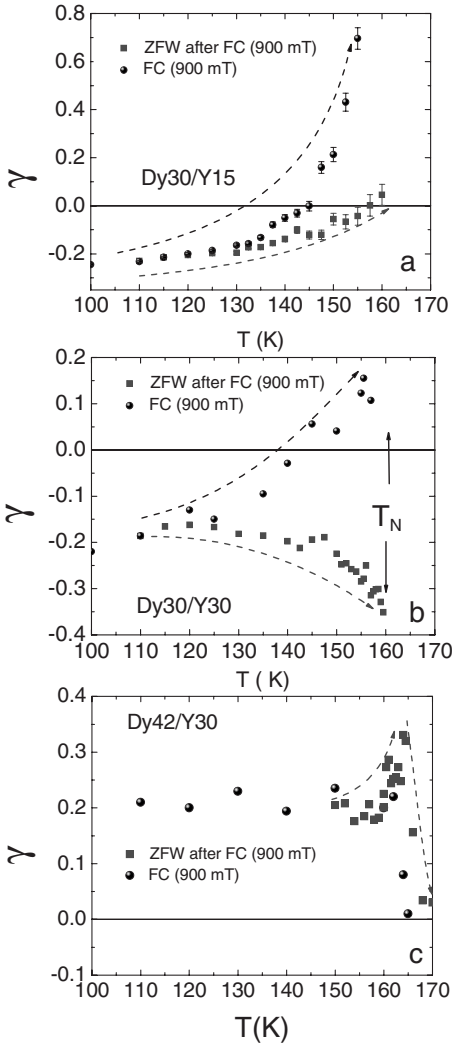

FIG. 4. The temperature dependence of the chiral parameter for three samples (a) Dy30/Y15, (b) Dy30/Y30, and (c) Dy42/Y30 for different temperature/magnetic field prehistory of the sample (closed circles—ZF warming after FC at $H=0.9$ T to $T=110$ K; open circles—FC in $H=0.9$ T to the temperature of interest T).

($T>T^*=145$ K) and low-temperature ($T<T^*$) regimes [Fig. 5(b)]. The sign of γ changes for the sample Dy30/Y15 [Fig. 5(a)] from negative in the low-temperature ($T=110$ and 130 K) to positive in the subcritical temperature regime ($T=150$ K). For all three samples the absolute value of $|\gamma|$ for low temperatures and large fields is in order of 0.2, although showing different signs. This implies that the field-induced chirality is an intrinsic property for the multilayer structures consisting of Dy/Y bilayers. The behaviors of the chirality for Dy30/Y15 and Dy30/Y30 are similar in the subcritical range which can attributed to the thickness of the Dy layer. It seems that the thickness of Y does play a role in the peculiarities of the chiral behavior of these two samples at low temperatures. Comparing the samples Dy30/Y30 and Dy42/Y30 it should be noted that the subcritical temperature dependences of γ are very similar while magnetic field dependences at low temperatures are different.

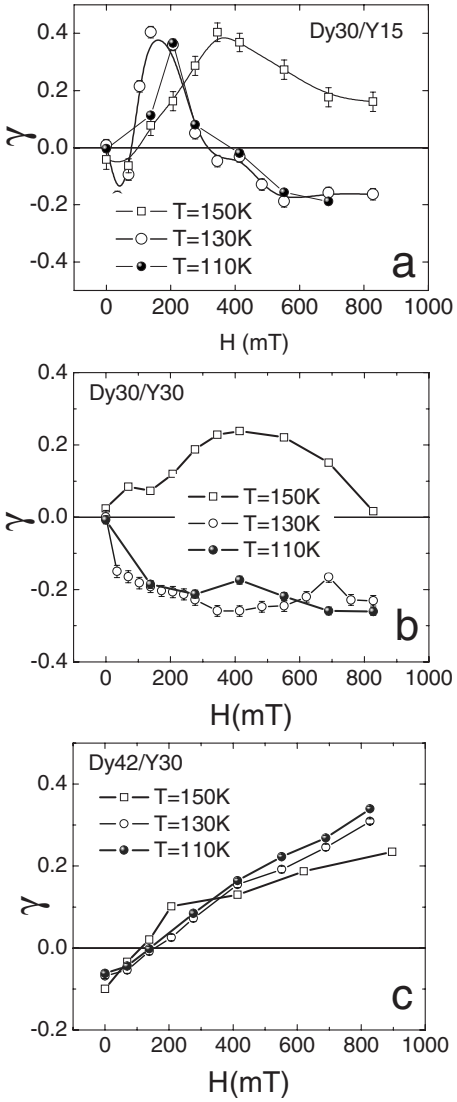

FIG. 5. The chiral parameter γ for three samples (a) Dy30/Y15, (b) Dy30/Y30, and (c) Dy42/Y30 as a function of the magnetic field H applied in the FC procedure to $T=150$ K, $T=130$ K, and $T=110$ K.

IV. INTERPRETATION

To interpret the obtained data one has to consider those interactions which determine the magnetic structure in the MMLs, as they were already mentioned in Sec. I. The major one is the RKKY interaction inside the Dy layers. It is responsible for the appearance of the helical spin structure which is the ground state of the magnetic structure for bulk Dy. As it was already pointed out above, the pitch angle of the helix decreases as the temperature decreases. The interlayer exchange between the Dy layers across the intervening Y is of similar origin than the RKKY intralayer coupling and couples the magnetic moments in the Dy layers at the vicinities of the Y layer. It is determined solely by $k_Y=3.1$ nm^{-1} and has a positive sign for $d_Y=3$ nm and a negative sign for $d_Y=1.5$ nm favoring a ferromagnetic and antiferromagnetic alignment of Dy spins, respectively, at the two interfaces for the different Dy/Y samples studied here. This second type of

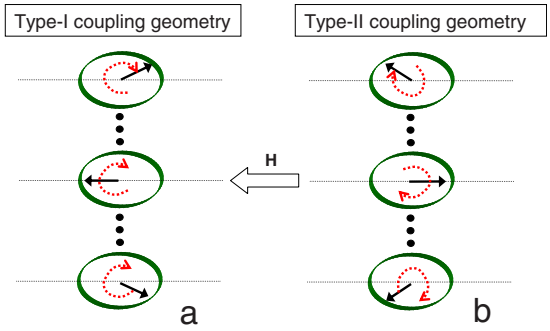

FIG. 6. (Color online) The type-I and type-II field-helix coupling geometry if (a) $d_{Dy}<2\pi/k_{Dy}$ or (b) $d_{Dy}>2\pi/k_{Dy}$, respectively. The black arrows indicate the direction of the magnetization in the planes at the center and at the interfaces of the Dy layers. The dashed arrows help one to visualize the helix, here with the left-handed chirality. The equivalent right-handed helix can be drawn since the field-helix coupling does not determine the sense of chirality.

RKKY interaction between the Dy layers provides the coherency of the helix that propagates throughout the bilayers. It is important to note that k_Y does not depend on the temperature. These two interactions produce a long-range coherent helix in MMLs but cannot break the chiral symmetry leading to different population number of left- and right-handed domains of the helices.

The chirality discussed in this paper is mainly induced by the in-plane applied magnetic field which interacts with the uncompensated moments of the Dy layer. The classical energy of this interaction can be simply evaluated by taking the integral of the magnetic contributions over the layer of the thickness d_{Dy},

$$F_H = -\int_0^{d_{Dy}} \mathbf{H} M_0 [\mathbf{e}_x \sin(k_{Dy} z + \phi_0) + \mathbf{e}_y \cos(k_{Dy} z + \phi_0)] dz,$$

where M_0 is the staggered magnetization of the Dy atomic layer, and ϕ_0 is the angle between the field and the moment at the Dy/Y interface, and $\mathbf{e}_x$ and $\mathbf{e}_y$ are the unit vectors along the corresponding axes. For $d_{Dy}<2\pi/k_{Dy}$ the energy F_H is minimized $[F'_H(\phi_0)=0]$ at an angle $\phi_0=\pm k_{Dy} d_{Dy}/2$. This means that the magnetization in the middle of the Dy layer, $\mathbf{M}(z=d_{Dy}/2)$, is parallel to the field axis (type-I coupling geometry) [Fig. 6(a)]. On the other hand, if $d_{Dy}>2\pi/k_{Dy}$ then the energy F_H is minimized at an angle $\phi_0=\pm(k_{Dy} d_{Dy}/2-\pi)$ and the magnetization in the middle of the Dy layer, $\mathbf{M}(z=d_{Dy}/2)$, is antiparallel to the field axis. The magnetization of the interface layers $\mathbf{M}(z\sim d_{Dy})$ and $\mathbf{M}(z\sim 0)$ are fixed at sharp angles with respect to the field axis (type-II coupling geometry). Depending on the type of the coupling geometry different parts of the Dy layers are in favor of the direction of the applied magnetic field, i.e., the middle part of the helix for the type-I geometry ($d_{Dy}<2\pi/k_{Dy}$) and the interfacial parts for the type-II geometry ($d_{Dy}>2\pi/k_{Dy}$). It should be noted that even though the helices drawn for illustrations in Figs. 6(a) and 6(b) are left handed, they could equivalently be shown as right-handed

ones because the field-helix interaction itself is chiraly neutral and does not break the symmetry.

Taking into account the parameters of the interactions, i.e., the RKKY interactions inside and between the Dy layers as well as the field-helix interaction in combination with the experimentally observed chirality γ, one can reconstruct the preferable spin structure inside the MMLs as a function of the temperature and the magnetic field. The principles of the reconstruction are as follows: (i) the chirality is degenerated inside the Dy layer so that the helix in the Dy layers can be equally left or right handed. The chirality within the layer is taken from the experiment. (ii) The dislocation of the spins at the two interfaces of two neighboring Dy layers (parallel or antiparallel) is determined by the interlayer RKKY interaction or, if the magnetic field is high enough, by the field-helix interaction. If the two interactions compete with each other the limiting cases need to be considered. (iii) The spin structure created under the applied magnetic field conserve its chirality upon reducing the field down to zero. In particular, the applied field helps to remove the domain walls in the helix structure within a Dy layer. This reconstruction aims to define the twist angle between the spins at the interfaces of two neighboring Dy layers for a given temperature and magnetic field prehistory. Given the twist angle, it determines the sign of the chiral interaction at the interfaces. Below we give several examples of such reconstruction.

The sample Dy42/Y30 has a positive field induced chirality for the whole temperature range below T_N which is ascribed to the right-handed preferable helix inside the Dy layers (see Fig. 4). Since d_{Dy} is larger than $2\pi/k_{\mathrm{Dy}}$ for the whole temperature range only the type-II coupling geometry applies for this sample. Further the RKKY interaction between the Dy layers prefers the ferromagnetic type of the spin alignment at the interfaces. Figure 7 shows the spin structure as it can be derived using above formulated principles. Here, in order to achieve a reasonable reconstruction, i.e., that repeating Dy/Y bilayers possess the same magnetic structure, the interface Dy moments need to be twisted in a particular direction. We emphasize that this twist angle between spins at two interfaces is here negative, showing the left-handed tendency for the dislocation of spins at the interfaces which is opposite to the right handedness of the helix inside Dy layer. This situation holds for all temperatures and magnetic fields [see Figs. 4(c) and 5(c)].

The type-II coupling geometry is also present for the sample Dy30/Y30 in the subcritical temperature range $T_N > T > T^* = 145$ K accompanied again by the positive sign of γ for all magnetic fields [see Fig. 5(b)]. The RKKY interaction between the Dy layers prefers again the ferromagnetic type of the spin alignment at the interfaces. Therefore the spin configuration for this temperature range is the same as shown in Fig. 7. However, the situation changes for low temperatures $T < T^*$. Here, d_{Dy} becomes smaller than $2\pi/k_{\mathrm{Dy}}$ which leads to the type-I coupling geometry. The transition is accompanied by the change in the sign of γ from positive to negative [see Figs. 4(b) and 5(b)] indicating that now the left-handed helices are dominant in the sample. The RKKY interaction between the spins at subsequent interfaces on the other hand does not change with temperature, remaining the ferromagnetic type. The spin structure of Dy30/Y30 changes

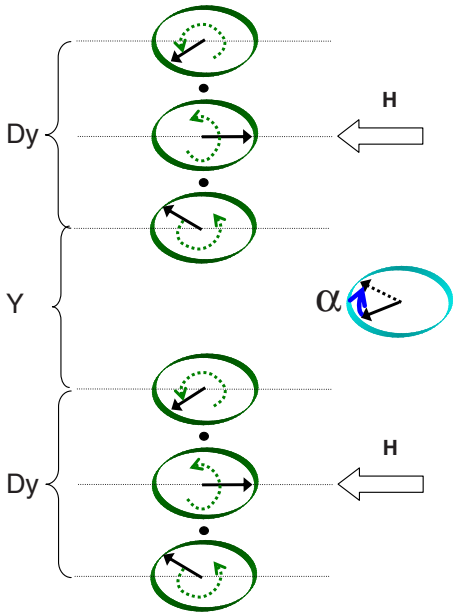

FIG. 7. (Color online) The visualization for the reconstruction of the spin structure in Dy42/Y30. The black arrows indicate the direction of the magnetization in the planes at the center and at the interfaces of two Dy layers. The right-handed chirality of helix inside a Dy layer is shown by the dashed arrows, corresponding to the positive sign of the field-induced chirality. The circle in the middle of Y layer shows the mutual close-to-ferromagnetic displacement of the magnetization at the two subsequent interfaces (Dy/Y and Y/Dy). In this configuration one derives a negative (left-handed) twist of the angle α between the two magnetizations. This spin structure is also realized in the subcritical temperature range for Dy30/Y30 and Dy30/Y15.

accordingly as shown in Fig. 8. We emphasize that now the spin chirality within the Dy layer is left handed in accordance to the experimental data but the twist angle between spins at two interfaces still remains negative, showing the same left-handed tendency for aligning the spins at the interfaces for the whole temperature range. This flip of the chirality with the temperature accompanied by the change in the field-helix coupling geometry demonstrates the mechanism of the coupling between the field and the chirality in the system. It should be noted that the change in the direction of the applied field in such a mechanism does not change the sign or the value of the chirality as it was indeed observed here in the experiment.

In the situation of the sample Dy30/Y15, the type-I field-helix coupling geometry is replaced by the type-II geometry at $T = T^* = 145$ K as already described for the sample Dy30/Y30. The sign of γ changes from negative at low temperature to positive close to T_N for large magnetic fields [Fig. 4(a)]. The spin structure can again be reconstructed as shown in Figs. 7 and 8 for the high- and low-temperature ranges, respectively. However, the situation here is more complex since the chirality γ is positive for low temperatures when the fields are relatively low [Fig. 5(a)]. This complex behavior is related to the fact that the interlayer RKKY interaction is of the antiferromagnetic type. For a low magnetic field, the field-helix coupling is also weak and the antiferromagnetic

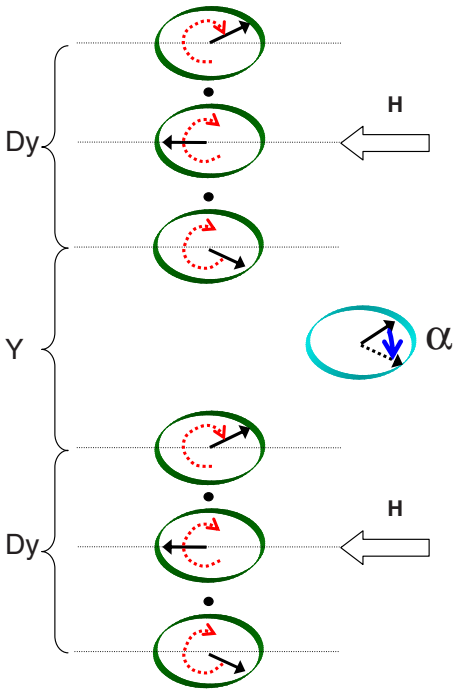

FIG. 8. (Color online) The visualization for the reconstruction of the spin structure in Dy30/Y30 similar to Fig. 7. Here, a left-handed chirality of helix inside a Dy layer is present indicated by the dashed arrows, corresponding to a negative sign of the field-induced chirality. Again a negative (left-handed) twist of the angle α between the two magnetizations is found. This spin structure is also realized in the low-temperature and high-field regime for Dy30/Y15.

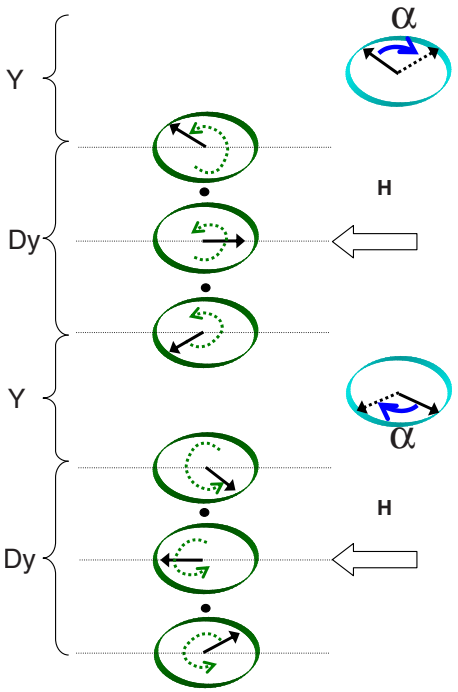

FIG. 9. (Color online) The visualization for the reconstruction of the spin structure in Dy30/Y15 for the low-field range $H<H_{tr}$ and low-temperature range $T<T^*$ (see also Figs. 7 and 8). Here, right-handed chirality of helix inside a Dy is observed indicated by the dashed arrows, corresponding to a positive sign of the field-induced chirality. As already shown in the other reconstructions the twist of the angle α between the two magnetizations is again negative (left handed).

interaction dominates due to the RKKY throughout the Y layer, i.e., the field-helix interaction can be neglected. The spin configuration for low temperatures and low fields is thus constructed accounting for the antiferromagnetic RKKY between the Dy layers and for the positive sign of the chirality inside the Dy layer. The reconstructed spin system is shown in Fig. 9. Here the required twist angle between spins at two interfaces is still negative. If now the field-helix coupling becomes stronger than the antiferromagnetic interaction due to RKKY, the type-I field-helix coupling geometry will be dominant in the system (Fig. 8). In this case the antiferromagnetic coupling due to the RKKY interaction can be neglected, which leads again to the spin configuration drawn in Fig. 7.

The main result of the reconstruction of the spin configurations for all samples is that the twist angle between the spins at two interfaces is always negative for all temperatures and magnetic fields. It can be therefore interpreted as a fingerprint of a new type of the antisymmetric interaction giving the left-handed twist for the magnetically coupled spins at the interfaces. It should be noted that, in principle, the chirality can be also induced if the magnetic field was applied after ZFC to a temperature below T_N. However, it was not possible for the sample Dy42/Y30 for magnetic fields up to 1 T. On the other hand, for the sample Dy30/Y15 and Dy30/Y30 chirality can be induced after ZFC, if the applied magnetic field exceeds the threshold value in the order of H_{tr}=300 mT or 400 mT, respectively. These values are close to that where the chirality γ changes its sign in the FC regime for Dy30/Y15 [see Fig. 5(a)], emphasizing the importance of the critical temperature range that should be passed through during the FC procedure. Upon ZFC a helix inside one Dy layer suffers from the domain walls between the right- and left-handed spiral structures, which cannot be removed at low temperature if the magnetic field is not high enough. If the magnetic field is applied upon cooling, it first removes the domain walls inside the Dy layer. Second, the field-helix coupling competes with the interlayer RKKY interaction. When the two interactions stabilizes the structure, the third antisymmetric DM interaction, appearing due to the lack of the symmetry inversion on the interfaces, reveals itself through the experimentally determined twist angle between the spin planes of the Y/Dy interfaces. The DM interaction reflects itself finally through the sign of the average chirality of the structure. One can conclude that the appearance of the chirality is strongly related to the critical temperature range where the softening of the magnetic structure allows the weak chiral force to induce the nonequal population of the left- and right-handed domains.

V. CONCLUSION

We have described the mechanism of the coupling of the in-plane applied magnetic field to the sign of the average chirality observed in three Dy/Y samples with different Dy

and Y layer thicknesses. Furthermore, we speculate that the spin chirality is caused by DM interaction, which stem from the noninverse exchange coupling close to the magnetic-nonmagnetic interfaces, similar to former findings at surfaces.[26,27] We also give further experimental evidence for the appearance of a DM type of interaction at the interfaces of the Dy/Y multilayer structure. This finding changes the whole concept of the magnetic structures in nanomagnetism as it introduces a new important DM interaction into the consideration of all nano-objects including the multilayer structures. The DM interaction presents a fundamental interaction in the theoretical considerations of the MMLs which leads to noncollinear spin arrangements at surfaces and interfaces.[28]

ACKNOWLEDGMENTS

The PNPI team acknowledges GKSS for their hospitality and financial support during the stay at GKSS. This work was performed within the framework of a Federal Special Scientific and Technical Program (Project No. 02.740.11.0874). The work is partially supported by RFFR under Project No. 09-02-01231.

*grigor@pnpi.spb.ru

[1] M. N. Baibich, J. M. Broto, A. Fert, F. Nguyen Van Dau, F. Petroff, P. Etienne, G. Creuzet, A. Friederich, and J. Chazelas, Phys. Rev. Lett. **61**, 2472 (1988).
[2] P. Grünberg, R. Schreiber, Y. Pang, M. B. Brodsky, and H. Sowers, Phys. Rev. Lett. **57**, 2442 (1986).
[3] P. Bruno and C. Chappert, Phys. Rev. Lett. **67**, 1602 (1991); **67**, 2592 (1991).
[4] V. Leiner, K. Westerholt, A. M. Blixt, H. Zabel, and B. Hjorvarsson, Phys. Rev. Lett. **91**, 037202 (2003).
[5] R. W. Wang, D. L. Mills, Eric E. Fullerton, J. E. Mattson, and S. D. Bader, Phys. Rev. Lett. **72**, 920 (1994).
[6] V. Lauter-Pasyuk, H. J. Lauter, B. P. Toperverg, L. Romashev, and V. Ustinov, Phys. Rev. Lett. **89**, 167203 (2002).
[7] J. Unguris, R. J. Celotta, and D. T. Pierce, Phys. Rev. Lett. **67**, 140 (1991).
[8] J. C. Slonczewski, Phys. Rev. Lett. **67**, 3172 (1991).
[9] A. Moser, A. Berger, D. T. Margulies, and E. E. Fullerton, Phys. Rev. Lett. **91**, 097203 (2003).
[10] A. Azevedo, C. Chesman, S. M. Rezende, F. M. de Aguiar, X. Bian, and S. S. P. Parkin, Phys. Rev. Lett. **76**, 4837 (1996).
[11] V. K. Vlasko-Vlasov, U. Welp, J. S. Jiang, D. J. Miller, G. W. Crabtree, and S. D. Bader, Phys. Rev. Lett. **86**, 4386 (2001).
[12] C. H. Marrows and B. J. Hickey, Phys. Rev. B **59**, 463 (1999).
[13] J. T. Kohlhepp, O. Kurnosikov, and W. J. M. de Jonge, J. Magn. Magn. Mater. **286**, 220 (2005).
[14] J. Kohlhepp, M. Valkier, A. van der Graaf, and F. J. A. den Broeder, Phys. Rev. B **55**, R696 (1997).
[15] K. Suenaga, S. Higashihara, M. Ohashi, G. Oomi, M. Hedo, Y. Uwatoko, K. Saito, S. Mitani, and K. Takanashi, Phys. Rev. Lett. **98**, 207202 (2007).
[16] A. N. Bogdanov and U. K. Rossler, Phys. Rev. Lett. **87**, 037203 (2001).
[17] A. Crépieux and C. Lacroix, J. Magn. Magn. Mater. **182**, 341 (1998).
[18] S. V. Grigoriev, Yu. O. Chetverikov, D. Lott, and A. Schreyer, Phys. Rev. Lett. **100**, 197203 (2008).
[19] M. B. Salamon, S. Sinha, J. J. Rhyne, J. E. Cunningham, and Ross W., Erwin, J. Borchers, C. P. Flynn, Phys. Rev. Lett. **56**, 259 (1986).
[20] R. W. Erwin, J. J. Rhyne, M. B. Salamon, J. Borchers, R. Du Shantanu Sinha, J. E. Cunningham, and C. P. Flynn, Phys. Rev. B **35**, 6808 (1987).
[21] F. Tsui, C. P. Flynn, M. B. Salamon, R. W. Erwin, J. A. Borchers, and J. J. Rhyne, Phys. Rev. B **43**, 13320 (1991).
[22] D. A. Jehan, D. F. McMorrow, R. A. Cowley, R. C. C. Ward, M. R. Wells, N. Hagmann, and K. N. Clausen, Phys. Rev. B **48**, 5594 (1993).
[23] I. E. Dzyaloshinskii, Zh. Eksp. Teor. Fiz. **46**, 1420 (1964) [Sov. Phys. JETP **19**, 960 (1964)].
[24] S. V. Maleyev, Phys. Rev. Lett. **75**, 4682 (1995).
[25] D. Lott, S. V. Grigoriev, Yu. O. Chetverikov, and A. Schreyer (unpublished).
[26] M. Bode, M. Heide, K. von Bergmann, P. Ferriani, S. Heinze, G. Bihlmayer, A. Kubetzka, O. Pietzsch, S. Blugel, and R. Wiesendanger, Nature (London) **447**, 190 (2007).
[27] E. Y. Vedmedenko, L. Udvardi, P. Weinberger, and R. Wiesendanger, Phys. Rev. B **75**, 104431 (2007).
[28] J. T. Haraldsen and R. S. Fishman, Phys. Rev. B **81**, 020404(R) (2010).